Contemporary Engineering Sciences, Vol. 4, 2011, no. 3, 101 - 117

Structural, Optical and Photoconductivity Studies of ZnO:As Nanocrystalline Thin Films

K. Saravanakumar

PG and Research Department of Physics
Kongunadu Arts and Science College
Coimbatore -29, India

C. Gopinathan and K. Mahalakshmi

PG and Research Department of Physics
The Madura College, Madurai – 625 011, India

V. Ganesan, V. Sathe

UGC-DAE Consortium for Scientific Research
Khandwa Road, Indore 452 017, India

C. Sanjeeviraja*

Department of Physics, Alagappa University
Karaikudi – 630 003, India

* Corresponding author
sanjeeviraja@rediffmail.com, saravanakumar_saran@yahoo.co.in

Abstract

Nanocrystalline ZnO:As films prepared using RF-Magnetron sputtering with different substrate temperatures. Structural study has done using x-ray diffraction (XRD) and the lattice parameter is affected to the lattice mismatch of As with Zn and O. we discussed mainly the changes in the optical and steady-state photoconductivity properties of ZnO with the inclusion of As atoms. Further the

change in the frequency modes are observed with the inclusion of As is identified with Raman Spectrum.

Keywords: As:ZnO, Raman Spectrum, Photoconductivity

1. INTRODUCTION

Zinc oxide (ZnO) is a II–VI n-type semiconductor with wurtzite structure with ions connected with four counter ions in the tetrahedral bond of sp^3 hybridization [1]. It has been widely studied because of its unique properties such as wide bandgap of 3.3 eV and large excitonic binding energy of 60 meV at room temperature [2].

The undoped ZnO thin films show n-type and already good for the device applications due to the native defects such as zinc intersitials and oxygen vacancies. However, the growth of p-type ZnO is having few difficulties and it is hindered the developments of blue/UV p-n junction light emitting diodes and Laser diodes. The most suitable dopants for p-type doping in ZnO are the group V elements (N, P & As) substituting for O, although the theory suggests difficulty in achieving shallow acceptor levels. Preparation of p-type ZnO has been successfully made with monodoping with (N,P) [3-5] and codoping [6,7] of by a large number of groups. But in contrast, there are few reports on the fabrication of As doped p-type ZnO films. This is because of the As ionic radius is larger than the O ionic raidus. If the As atom substitutes in ZnO lattices, it will produce lattice defects in adjacent sites.

The researchers are giving more attention on the electrical properties of As doped ZnO for the fabrication of p-type ZnO. Optical properties are very important to fabricate high quality optoelectronic devices. Here we discussed mainly the changes in the optical and steady-state photoconductivity properties of ZnO with the inclusion of As atoms. As doped nanocystalline films are giving more attention because the reduction of particle size novel electrical, mechanical and optical properties are introduced, which are largely believed to be the result of surface and quantum confinement effects.

For making the zinc rich environment in the preparation conditions for the possibility of substituting the As in O position because to avoid the bonding of As and O, we have tried ZnO nanocrystalline films in the absence of oxygen atmosphere on glass substrates prepared using RF magnetron sputtering technique. And we discussed the effects of substrate temperature on the growth of highly textured nanocrystalline ZnO:As thin films on glass substrates.

2. EXPERIMENTAL

Thin films were prepared by planar RF-magnetron sputtering from ZnO:As (3 Wt%) target. The target was prepared by mixing and grinding the powders of ZnO (99.99%, Merck) and As_2O_3 (99.99%, Merck) using the ball mill for 20 hours. Then the prepared target is palletized to a diameter of 50 mm and 5 mm thickness and sintered at a temperature of 950°C. The substrate was set at a distance of 6 cm above the target. Corning 7059 glass plates were used as substrate. Before deposition, the chamber was evacuated to an ultimate background pressure of 10^{-6} mbar for 1 h and pre-sputtering process employed for 10 min to clean the target surface. High purity Ar (99.999%) was used as sputtering gas. The Ar flow was introduced directly into dark space shields of the sputtering sources. The sputtering gas pressure was controlled by adjusting a needle valve and the deposition pressure in the chamber was maintained at 10^{-4} mbar. Substrate temperature was varied from room temperature (RT) 27 to 300ºC, and the RF power was maintained at 200W.

The structure and phase purity characterization of the films was carried out with a Rigaku X-ray diffractometer using CuK_α radiation. The optical transmittance of the films was studied using a UV-Vis-NIR spectrophotometer (Ocean-Optics Inc., HR2000 Model) with a cleaned corning glass in the reference beam. Raman measurements of these samples were performed using Horiba Jobin Yvon LABRAM-HR spectrometer with an excitation wavelength of 400 nm in the back scattering geometry at room temperature. The d.c conductivity and photoconductivity measurements were done with the help of standard two-probe technique and Keithley 614 programmable digital electrometer. For illuminating the sample commercially available LED is used which can emit white light in the visible region. The power supply to the LED is kept outside the cryostat whereas the LED was kept just above the sample in order to utilize its full illumination. The whole set up is then placed in cryostat and vacuum (10^{-5} mbar) is provided with diffusion – rotary assembly.

3. RESULTS AND DISCUSSION

3.1 FILM STRUCTURE

Fig. 1 shows the XRD patterns of the As doped ZnO thin films deposited at 27, 100, 200, 300 and 400 ^oC substrate temperatures. All films show a pronounced (002) peak around 34.32° for wurtzite structure of ZnO, indicative of preferential orientation with the *c* axis perpendicular to the substrate surface. The mean crystallite sizes (D_{XRD}) were calculated using the Scherrer formula, $D_{XRD}=0.94\lambda/(\beta \cos \theta_\beta)$, where λ, θ_β, and β are the x-ray wavelength, Bragg diffraction angle, and the line width at half maximum of the diffraction peak,

respectively. The mean crystallite size values and lattice constant values are given in table 1.

When the substrate temperature is increased from 27 to 200ºC, the 2θ peak position moved to lower angle side. It is due to the increase of lattice constant in c-axis. Atomic radius of As atom (1.20Å) is higher than O (0.73Å) and Zn (0.72Å) and the solubility of As atom in ZnO crystallite is low at RT [8]. The ionic radius of As is greater than Zn and O ionic radius and it is reported that the diffusion behavior of Ag having the same ionic radius as As in ZnO thin film is restricted at low temperature on below 175°C [8]. At these temperatures it may formed interstitial defects or As_2O_3 precipitate in ZnO matrix. It is already reported that the As would preferably bind with O more strongly than themself [9]. When further increasing of substrate temperature from 200°C, the peak position shift back to higher angle side and the c-axis lattice constant was get decreased. This may be explained that the As should either substituted in the zinc position or in the oxygen position.

It is noticed that the peak position of the film deposited at 400ºC is showing asymmetry with the reduction in intensity and the peak was blewup at the low angle side indicates the poor orientation and crystallinity of the film.

3.2 OPTICAL STUDIES

Fig. 2 is a transmission spectra of RF sputtered ZnO films. All films showed >85% transmission in the visible region. The absorption edge was not clearly visible. Interference pattern indicates that the film would have excess zinc sites at the grain boundaries which reflect the light intensity. The absence of interference pattern in the film deposited at 400^{o}C was due to the formation of grainy surface leading to large scattering loss [10].

Figs. 3 (a,b,c,d & e) show $(\alpha h\gamma)^2$ plots of ZnO:As films as a function of photon energy ($h\gamma$) to measure the optical bandgap (E_g). The E_g values were calculated using Tauc plot [11] as shown in the inset of figure 4, by extrapolating the linear line cut at the x-axis and the corresponding values are given in table 1.

Fig. 4 shows the variation of the bandgap of ZnO:As with respect to the substrate temperature. It is observed that the band gap of the film increasing upto 200^{o}C due to the increase of density of localized states in the forbidden gap effectively pins the Fermi level. Increasing the temperature above 200^{o}C, the intrinsic defects increases due to the oxygen deficiency in the preparation condition increases the carriers in the matrix and decreases the bandgap.

3.3 PHOTOCONDUCTIVITY

The temperature dependence of the dark- and steady-state photoconductivity and dark conductivity was measured in a vacuum (10^{-5} mbar) environment from 300 to 400 K. The heating and cooling rates were chosen in order to avoid thermally stimulated currents. White light is used with a photon flux varying from 5 x 10^{15} to 10^{17} photons/cm^2. It was checked that no space charge was created in the samples under illumination.

The d.c conductivity was measured as a function of temperature from 300 to 400 K. The results of these measurements are plotted as Fig. 5. It is clear from the figure that σ_{dc} Vs 1000/T curves are straight lines for most samples.

The d.c conductivity can, therefore be written as

$$\sigma_{dc} = \sigma_o \exp(-\Delta E/kT)$$

where ΔE is the thermal activation energy for d.c conduction and k is the Boltzmann's constant.

From the table 1, it is seeing that the As atoms is increasing the activation energy in turns decreasing the conductivity. Impurities and defects in semiconductors create defect-localized states that are located either in the bandgap, or resonant with in the continuum of the host bands. If such a defect level is occupied, it usually does not lead to conductivity due to the localized nature of the state and the ensuing high activation energy. As we discussed in structural studies the ionic radius of As atom relatively higher and soluble at a temperature above 175°C [8]. So it may form interstitial defects or the formation of As_2O_3 precipitate in ZnO crystallites inturns it creates localized states in the bandgap and decreases the conductivity as shown in Fig. 4. And after 200^0C it is expected that the As would mostly dissolved into the ZnO matrix and introduce an acceptors in the matrix. The charge neutralization takes place due to the recombination of donors with acceptors which in turn decreases the conductivity as well as increases the activation energy.

And above 300^0C, the conductivity again started to increase because of the intrinsic defects such as oxygen vacancies and interstitial zinc atoms. It is reported that the oxygen vacancies are the main contribution for the photoconduction in ZnO. The arsenic impurity in ZnO lattices present in a deep localized states and also in a delocalized states. Under the illumination of light, electron photoconduction takes place and it decreases at higher temperature because of the delocalized As atoms becomes localized and it introduce a carriers and suppress the electron photoconductivity. Hence, the photosensitivity (σ_{ph}/σ_{dc}) is decreasing with the inclusion of As atoms. Here the As atoms tuning the photoconductivity of ZnO.

3.4 RAMAN STUDIES

Wurtzite type ZnO belongs to the C_{6v} ($P6_3mc$) space symmetry. Each unit cell is having 4 atoms and occupying 2b sites of symmetry C_{3v}. At the point near the Brillouin zone the following optical phonon modes are allowed, $\Pi_{opt} = A_1+2B_1+E_1+2E_2$. Among these, doubly degenerate B_1 modes are silent, A_1 and E_1 branches are both Raman and infrared active, and other doubly degenerate E_2 modes are Raman active. Figure 6 shows the Raman spectra of ZnO films grown at RT and 400ºC. Appearance of the peak near 275 cm^{-1} was attributed to the B_1 silent inactive mode. Raman active phonon mode E_2 (TO) was observed near to 438 cm^{-1}. Another mode observed around 580 cm^{-1} attributed to E_1 (LO) branch. The optical phonon modes confirm that the synthesized nanocystalline films have the wurtzite hexagonal phase. The E1 peak itself is enhanced compared to other peak positions while increasing the substrate temperature to 300^oC. Many researchers have found that the Raman mode at this peak position corresponds to silent modes [12]**,** Nitrogen-related vibrational modes [13] and defect associated with zinc interstitials, oxygen vacancies or their combination [14]. In our case, the appeared peak is due to the native defects produced in the film with the incorporation of As elements. There is no additional vibration peak found related to As. This may be because of the peak silent due to the metallic nature.

There is a shift found in E_1 phonon mode peak with respect to the standard value of 580 cm^{-1}. It is clearly indicating the tensile stress acting on the film and it is relaxing at a substrate temperature above 200^oC. There is no E_2 and B_1 peaks of phonon modes have found above 200^oC substrate temperatures.

3.5 Conclusion

In summary, high-quality ZnO:As films have been successfully grown on the glass substrate by the RF-Magnetron sputtering technique with different substrate temperatures. Structural study shows the lattice parameter is affected because to the lattice mismatch of As with Zn and O. Inclusion of As in ZnO:As increase the density of localized states in the forbidden gap and results effectively pins the Fermi level. Steady-state photoconductivity results shows the As element can effectively alter the photoconductivity of ZnO:As films. Raman spectra shows the tensile stress is acting on the ZnO:As films and the phonon peak related As is disappeared here due to the low concentrations or with the metallic nature.

References

[1] M. Tsukada, H. Adachi, C. Satoko, Prog. in Surf. Sci. 14 (1983) 113.

[2] Yoshitaka Nakano, Takeshi Morikawa, Takeshi Ohwaki and Yasunori Taga Appl. Phys. Lett. 88 (2006) 172103.

[3] J. Lu, Y. Zhang, Z Ye, L. Wang, B. Zhao and J. Huang, Mater. Lett. 57 (2003) 3311.

[4] M. Joseph, H. Tabata, H. Saeki, K. Ueda and T. Kawai, Physica B, 140 (2001) 302.

[5] K. Kim, H.S. Kim, D.K. Hwang, J.H. Lim and S.J. Park, Appl. Phys. Lett. 83 (2003) 63.

[6] H.P. He, Z.Z. e, F. Zhuge, Y.J. Zeng, L.P. Zhu, B.H. Zhao, J.Y. Huang and Z. Chen, Solid State Communications, 138 (2006) 542.

[7] J.M. Bian, X.M. Li, X.D. Gao, W.D. Yu and L.D. Chen, Applied Physics Letters, 84 (2004) 541.

[8] Hong Seong Kang, Byung Du Ahn, Jong Hoon Kim, Gun Hee Kim, Sung Hoon Lim, Hyun Woo Chang and Sang Yeol Lee, Appl. Phys. Lett. 88 (2006) 202108.

[9] Sukit Limpijumnong, S.B. Zhang, Su-Huai Wei and C.H. Park, Physical Review Letters, 92 (2004)1555504.

[10] P.M. Ratheesh Kumar, C. Sudha Kartha, K.P. Vijayakumar, T. Abe, Y. Kashiwaba, F. Singh and D.K. Avasthi, Semicond. Sci. Technol. 20 (2005) 120.

[11] J. Tauc, Amorphous and Liquid Semiconductors, plenum, New York, Ch. 4.

[12] F.J. Manjon, B. Mari, J. Serrano and A.H. Romero, J. Appl. Phys. 97 (2005) 053516.

[13] A. Kaschner, U. Haboeck, M. Strassburg, M. Strassburg, G. Kaczmarczyk, A. Hoffmann, C. Thomsen, A. Zeuner, H.R. Alves, D.M. Hofmann and B.K. Meyer, Appl. Phys. Lett. 80 (2002) 1909.

[14] Z.Q. Chen, A. Kawasuso, Y. Xu, H. Naramoto, X.L. Yuan, T. Sekiguchi, R. Suzuki and T. Ohdaira Phys. Rev. B 71 (2005) 115213.

Table 1 : Structural, optical, and photo-conducting properties of ZnO:As films with different substrate temperatures

Sub. Temp. (^oC)	Lattice parameter c (Å)	Optical bandgap (eV)	σ_d at RT $(\Omega cm)^{-1}$	E_a^d >RT (eV)		σ_{ph} at RT $(\Omega cm)^{-1}$	E_a^{ph} >RT (eV)		Sensitivity σ_{ph}/σ_d	E_a^{ph}/E_a^d
27	5.21	3.171	301.62	0.3047	-	398.104	0.3165	-	1.319	1.038
100	5.22	3.217	77.58	0.4531	-	98.278	0.3927	-	1.266	0.867
200	5.24	3.392	0.08105	0.7591	-	0.099	0.6549	-	1.221	0.863
300	5.23	3.321	1.0645	0.0759	0.0336	1.372	0.1400	0.0391	1.288	-
400	5.22	3.296	40.882	0.0350	-	54.163	0.0327	0.1094	1.325	-

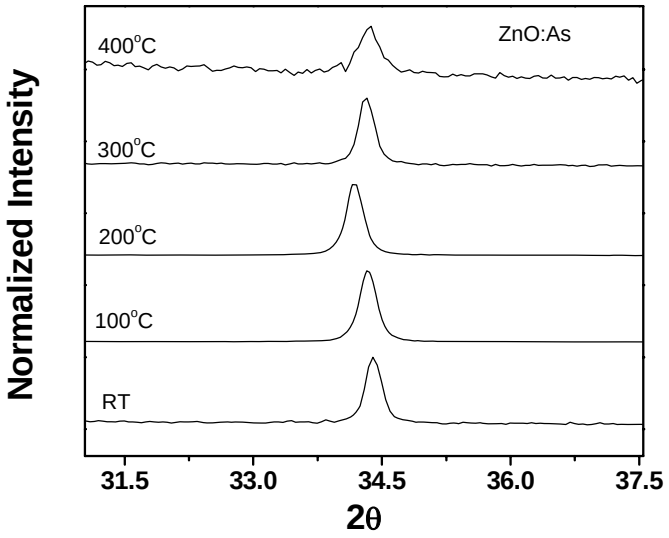

Fig. 1 XRD diffraction patterns of ZnO films grown on glass substrate for various temperatures

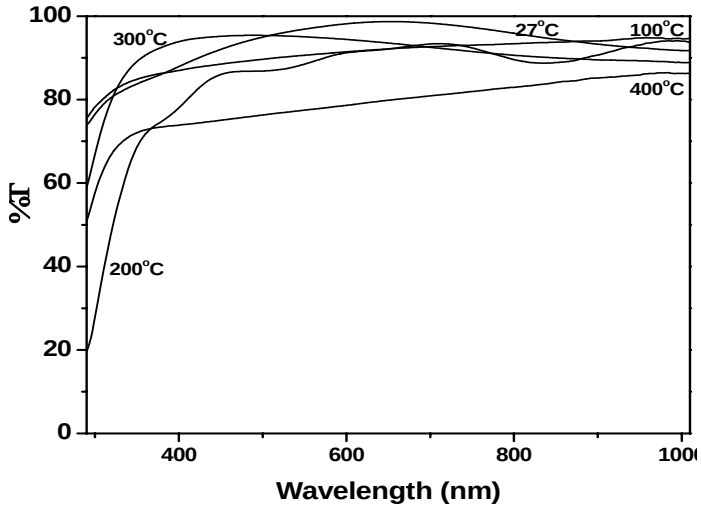

Fig. 2 Transmittance spectra of ZnO:As films measured at room temperature

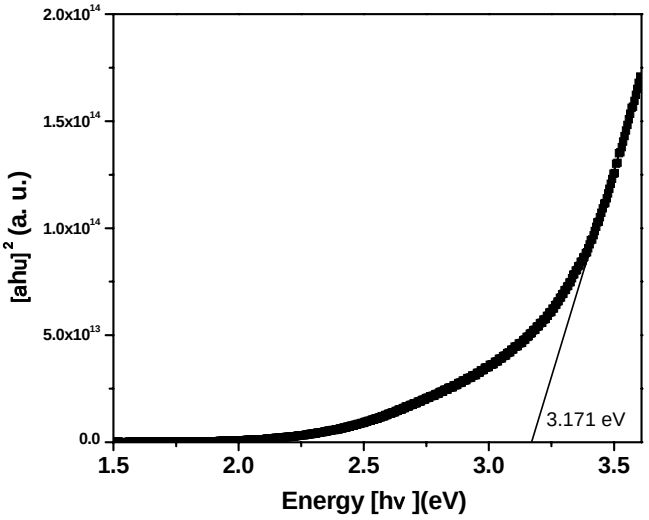
2.0x10^14
1.5x10^14
1.0x10^14
5.0x10^13
0.0
[ahu]^2 (a. u.)
1.5
2.0
2.5
3.0
3.5
Energy [hv](eV)
3.171 eV

(a)

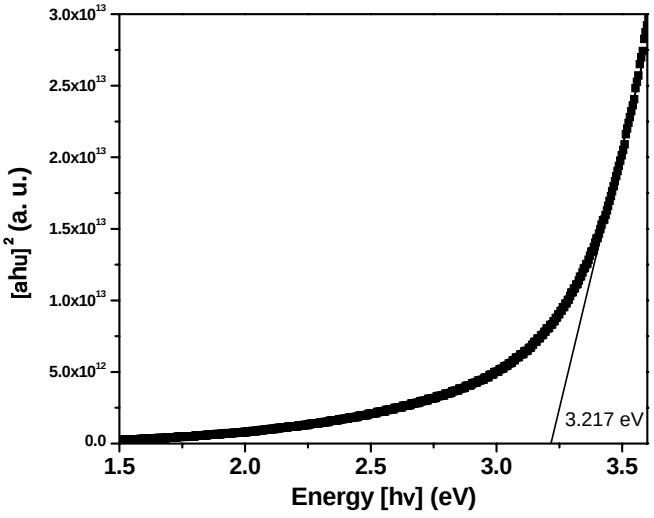
3.0x10^13
2.5x10^13
2.0x10^13
1.5x10^13
1.0x10^13
5.0x10^12
0.0
[ahu]^2 (a. u.)
1.5
2.0
2.5
3.0
3.5
Energy [hv] (eV)
3.217 eV

(b)

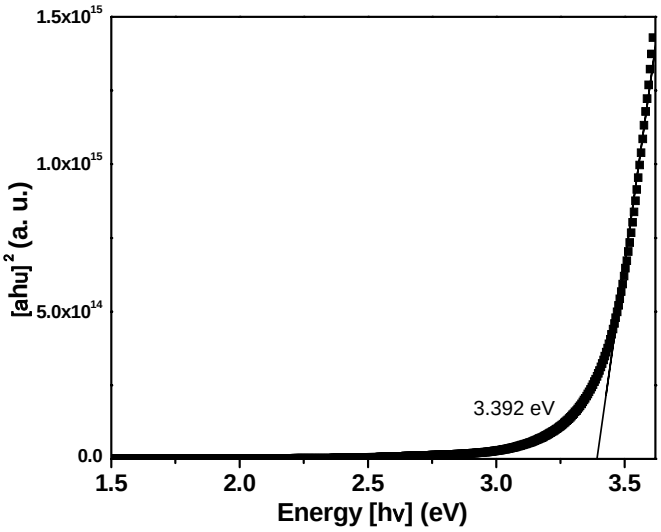
1.5x10^15
1.0x10^15
5.0x10^14
0.0
[ahu]^2 (a. u.)
3.392 eV
1.5
2.0
2.5
3.0
3.5
Energy [hv] (eV)

(c)

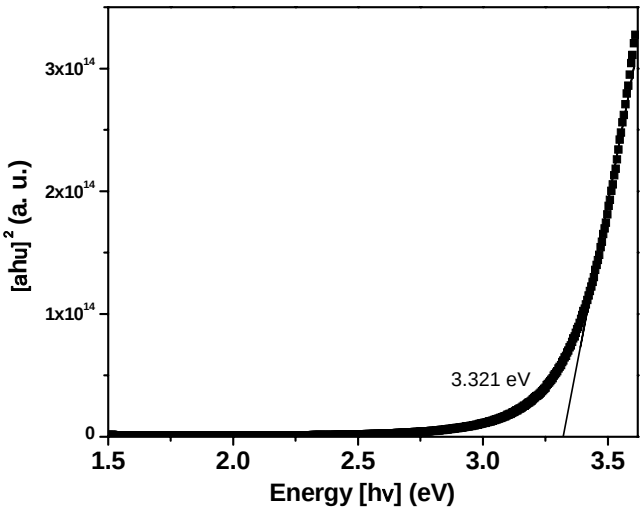

(d)

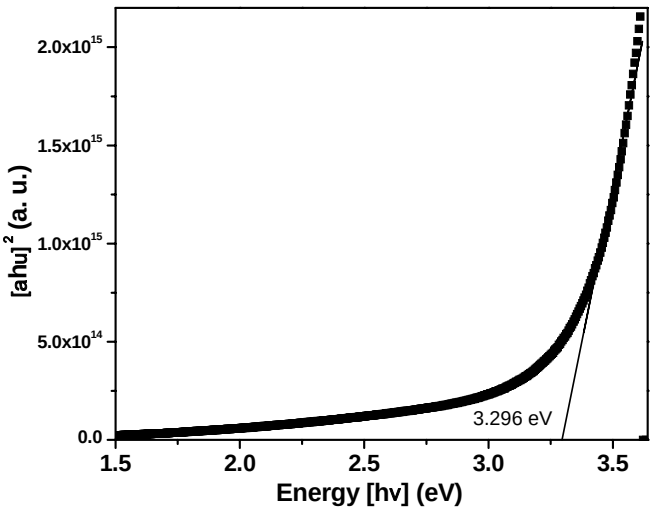

(e)

Fig. 3 Variation of $(\alpha h\gamma)^2$ of ZnO:As films as a function of photon energy ($h\gamma$) grown at a temperature of (a) 27, (b)100, (c) 200, (d) 300 and (e) 400 ºC.

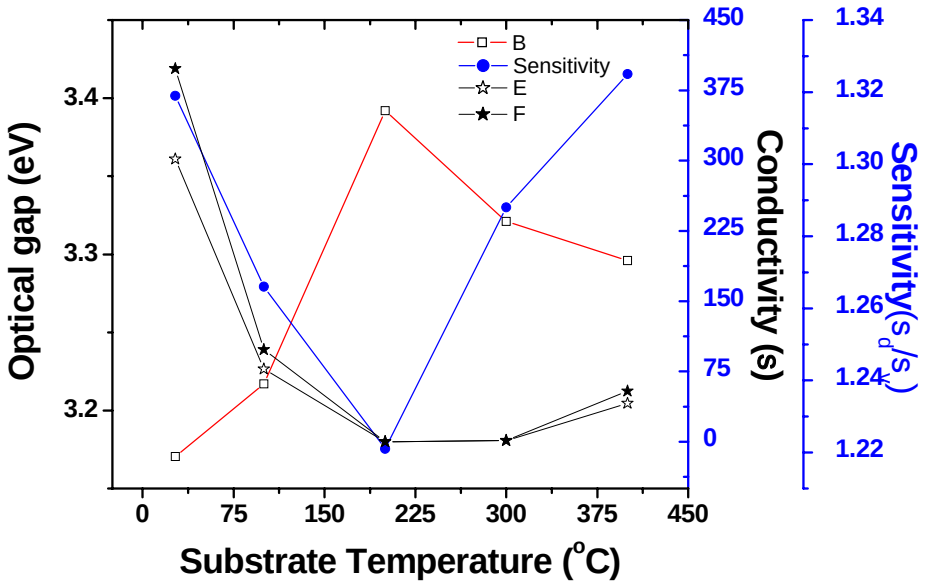

Fig. 4 Variation of Optical gap, conductivity and photosensitivity with respect to substrate temperature

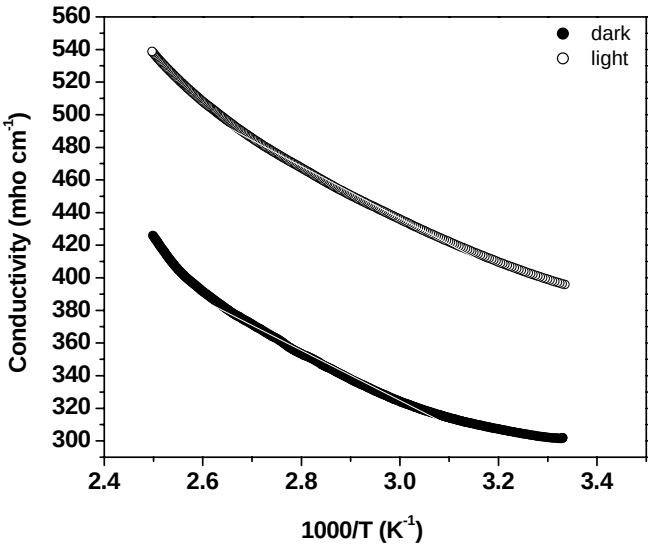
dark
light
Conductivity (mho cm-1)
1000/T (K-1)
560
540
520
500
480
460
440
420
400
380
360
340
320
300
2.4
2.6
2.8
3.0
3.2
3.4

(a)

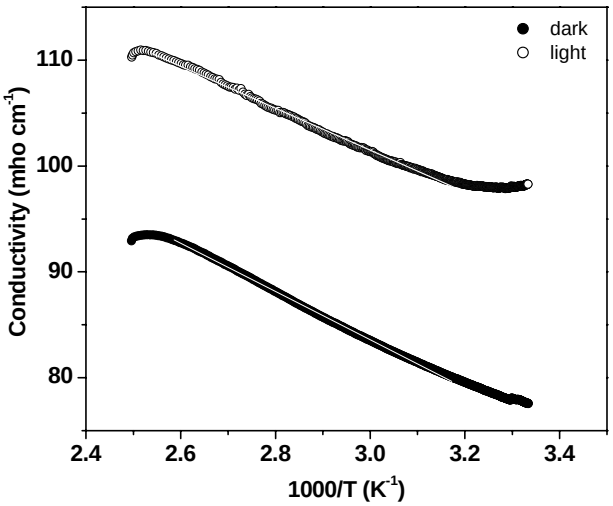
dark
light
Conductivity (mho cm-1)
1000/T (K-1)
110
100
90
80
2.4
2.6
2.8
3.0
3.2
3.4

(b)

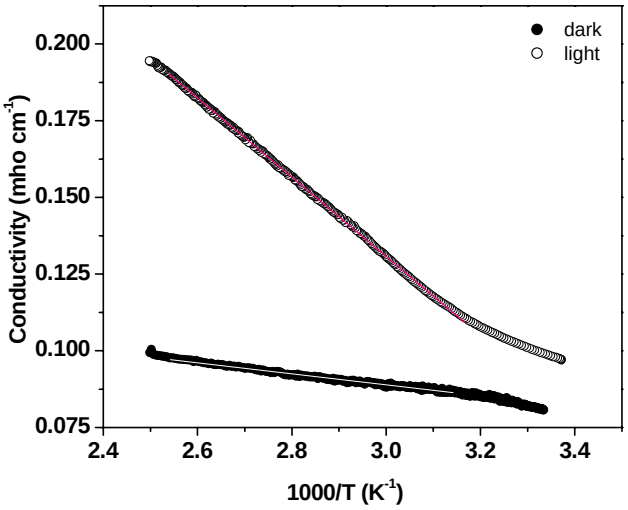
dark
light
Conductivity (mho cm-1)
0.200
0.175
0.150
0.125
0.100
0.075
2.4
2.6
2.8
3.0
3.2
3.4
1000/T (K-1)

(c)

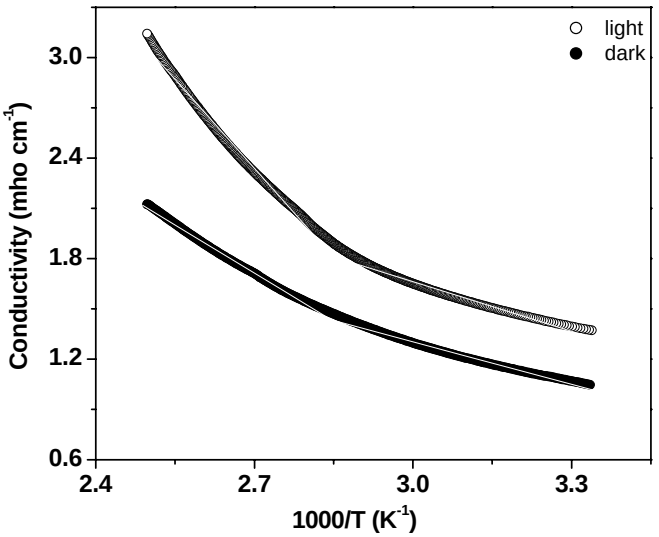

(d)

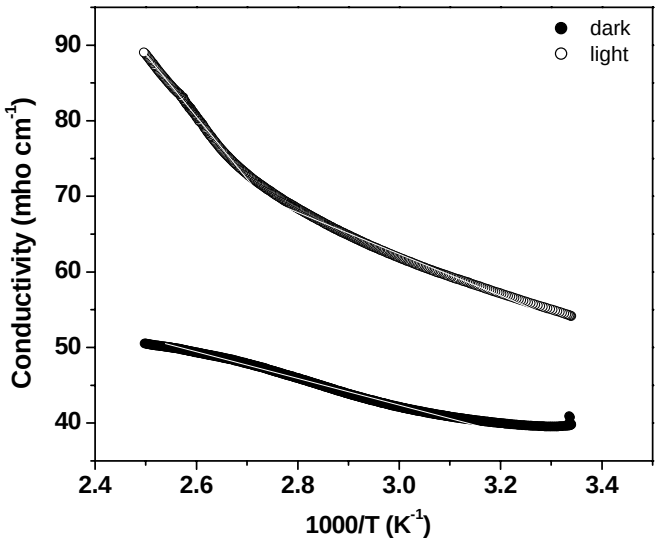

(e)

Fig. 5 Variation of dark- and steady-state photoconductivity with temperature for ZnO:As films grown at (a) 27, (b)100, (c) 200, (d) 300 and (e) 400 ºC.

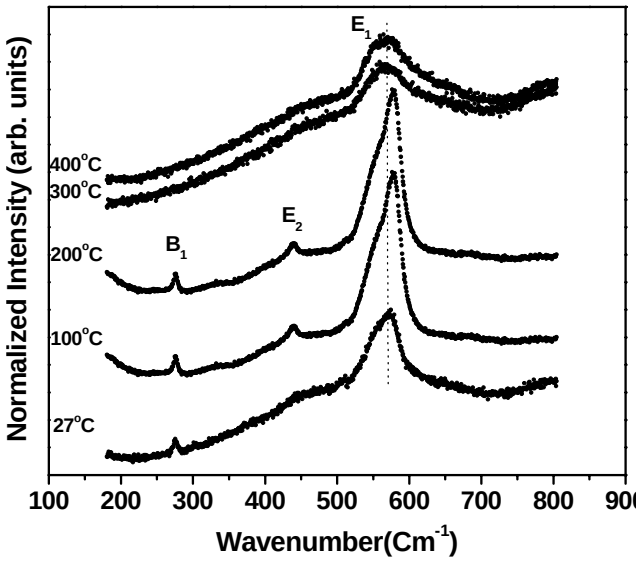

Fig. 6 Raman spectra of ZnO:As films grown at different substrate temperatures measured at room temperature.

Received: December, 2010